Chapter-5

Synthesis, characterization and application of PVC/Nano-bentonite composite membrane

This chapter deals with the synthesis of high performing antifouling polymeric membrane for the membrane separation processes for desired applications using polyvinyl chloride as base polymer, polyvinyl pyrrolidone as amphiphilic antifouling additive and hydrophilic bentonite nano clay as dispersed inorganic phase using non-solvent induced phase inversion process. To understand the effect of grafting nanoparticles and to support its antifouling nature, analysis of improved surface and mechanical properties of pure polyvinyl chloride membrane and all other composite membrane samples was done using scanning electron microscope, energy-dispersive x-ray spectroscopy, x-ray diffraction, drop shape analyzer and ultimate tensile machine . Surface morphology of modified membrane in terms structure, size, hydrophilicity, thermal and mechanical stability of membrane as well as flow parameters for pure water flux were studied. Experiments were carried out to study the performance of composite membranes.

5.1 Introduction

The efficiency of membrane separation processes depends on the selected membrane material, preparation method and operating conditions. Membrane Fouling is a major concern for a membrane manufacturer, which can critically reduce the membrane performance. Fouling is the phenomenon in which particles, macromolecules, salts and so forth get deposited at the surface of membrane or within the pores matrix. It may diminish the membrane flux temporarily as well as permanently. Temporary fouling can be restored mechanically by applying back-pressures to wash the membrane to

rejuvenate the initial flux. However, no technique can recover the permanent fouled membrane (Rana et al., 2010). In general, membrane material with high hydrophilicity is preferred to decrease the temporary fouling. However, hydrophilic polymeric materials lack the desired mechanical properties which are also very much essential to sustain the membrane during the backwashing and air flushing to rejuvenate temporary fouled membrane. For this reason, a major concern is to prepare a membrane with high hydrophilicity with improved mechanical properties for its potential application in industrial and municipal requirements.

Various researchers have used above technique to prepare porous polymeric mix matrix membranes using many different nanomaterials to investigate their effect on antifouling properties and performance of the membrane. Incorporation of these nanomaterials affects the pore structure, hydrophilicity, surface morphology and strength which in turn results in better performance and antifouling nature of membrane (Huang et al., 2012; Jafarzadeh et al., 2015; Maximous et al., 2009; Saleh et al., 2012; Shokri et al., 2016; Wu et al., 2015; Zhang et al., 2011).

Many researchers have reported work on the fabrication of polyvinyl chloride membranes using PVC. However, no such work has been published in the literature using polyvinylpyrrolidone (PVP) embedded Bentonite nano clay for enhancement of antifouling properties of the membrane.

The properties of PVC and the advantages of using it for the [reparation of composite membranes have been described in chapter 4.

Bentonite Clay minerals are hydrated phyllosilicates and may also be considered as hydroxides of silicon and aluminum. So far, quite a few studies have been done on preparing polymer-based composites using clay fillers and few researchers have also used such composites to prepare membranes using different polymers (Anadão et al.,

2010; Bergaya et al., 2013; Ghaemi et al., 2011; Pavlidou et al., 2008; Taghaddosi et al., 2017). PVP is synthetic hydrophilic, water-soluble and biodegradable polymer and it deserves a unique attention among the conjugated polymers due to its easy processibility, moderate electrical conductivity and rich charge transport mechanism. Humic acid (HA) is one of the major constituents of natural organic matter present in surface water. These elements are hazardous to human health and can cause dizziness and headache. It can also hamper central nervous system for a short period. Since it is so harmful to human health, it becomes essential to remove HA from water to mitigate its effect on human health (Huang et al., 1994; Waller et al., 1998).

5.2 Materials and Methods

5.2.1 Materials

Polyvinyl chloride (MW=80000) and Hydrophilic Bentonite nano clay (HB) was supplied by Sigma-Aldrich. Polyvinyl Pyrrolidone was bought from HPLC, Mumbai and used as pore former. N, N-Dimethylacetamide, used as polymer-solvent was purchased by Spectrochem, Mumbai. All chemical and reagents were used as purchased without any further modification and treatment.

5.2.2 Preparation of composite membrane

Non-solvent induced phase separation process was adopted for preparing Hydrophilic Bentonite grafted composite polyvinylchloride membranes in lab (Pezeshk et al., 2012). First, a known amount of HB was dispersed in DMAc and sonicated for 2 hours to have a homogenous suspension for a polymeric solution. Then pore former PVP was mixed to the solution and the solution was stirred at room temperature for 2 hours. Subsequently, PVC was added to solution and mixed by constant stirring for a day until the solution gets homogenous completely. After this the solution was further sonicated

to remove trapped air bubble in solution and casted with casting knife on a glass plate. After casting, the glass plate was immediately immersed in a deionized water bath, which works as non-solvent and phase inversion takes place and membranes were formed which were easily detached from the plate. Then membrane was immersed in distilled water for 48 hours for complete exchange of solvent DMAc. Membranes are dried and stored for further use. In this experiment, 5 different samples of various HB composition and constant polymeric concentration in all casting solution were 20%. The composition of all membrane samples is given in table 5.1.

Table 5.1: Composition of the membrane samples.

Membrane	DMAc (wt %)	PVC (wt %)	PVP (wt %)	HB (wt %)
M1	80	19	1	0
M2	79.5	19	1	0.5
M3	79.0	19	1	1.0
M4	78.5	19	1	1.5
M5	78.0	19	1	2.0

5.2.3 Characterization methods

The scanning electron microscope was used to visualize the morphology of membrane surface. All the analysis is done using instrument EVO - Scanning Electron Microscope MA15 /18, CARL ZEISS MICROSCOPY LTD. Since the sample is non-metallic, it is coated with gold before observation. Energy-dispersive X-ray spectroscopy (EDS) was used to verify the presence as well as the dispersion of HB within the membrane. For this purpose 51N1000 – EDS System, CARL ZEISS MICROSCOPY LTD is used. The other characterization techniques involved and the instrument details are same as used for PVC/Alumina composite membranes and have been discussed in chapter 4, section 4.2.3.

5.2.4 Performance study and antifouling analysis

Performance of pure PVC membrane and PVC/Bentonite composite membrane were further studied on a self-made dead-end lab-scale filtration setup to separate humic acid solution. Flux studies and antifouling analysis of membranes were done using the methodology as discussed in section 3.3.

5.3 Result and discussions

5.3.1 SEM and EDS analysis

SEM was used to study the change in surface morphology of neat PVC membrane with hydrophilic Bentonite. The SEM images showed the expected asymmetric structure on the surface of the membrane. Pores were observable in the entire membrane surface. It can be seen in the SEM images of figure 5.1 that M1 has denser structure and effect of the addition of HB could be easily seen in the images. Addition of dopant had made the surface rougher than the pure PVC membrane. It was observed that by adding filler, clusters were formed within membrane surface. With increasing the filler amount surface becomes more irregular and looks stronger with multilayer formation because of fillers. However, in M5 surface looks totally distorted with large numbers of layers in surface and huge cluster appears on the surface which supports XRD data of sample too. Furthermore, this could also be seen in the figure 5.1 that all the polymeric membranes synthesized had the macro-void structure, which can be because of the instantaneous de-mixing that might have occurred during phase inversion process because of total miscibility between DMAC and non-solvent, i.e. DI water. When the different amount of dopant was added in the preparation, the difference in macro voids was also seen on the surface of the membrane. These may be because of the fact that hydrophilic Bentonite gives faster affinity to water during phase inversion process.

When the casted membrane was immersed into the non-solvent during the phase inversion, the hydrophilic additives, as well as water-soluble PVP, had a tendency to leach out into the non-solvent and retain the non-polar PVC on the non-woven sheet. Therefore asymmetric pores were formed. Because of polymer-polymer interaction between PVC and PVP, some part of PVP could remain in the polymer matrix even after keeping the sheet in non-solvent for a long time. When HB particles were doped in the mixture, there must have been some interaction between HB and PVP. Since HB was hydrophilic, it would also try to move out during phase inversion through the surface and pores of the membranes. Since PVP was amphiphilic, it would bind the PVC matrix as well as holds the HB within the polymeric phase. Thus, the process results in increased porosity and enhancement in permeate flux. However, as the amount of HB increased, it could stay more in the polymer matrix and could be placed in the pores within the structure. It furthermore would resulted in the more significant amount of particles leaching out in the process and creating macro voids as shown in SEM images of M4 and M5 in figure 5.1. This also could affect the porosity of the membrane as a large amount of dopant, setting agglomerated in the membrane, would increase the viscosity of the casting solution and in turn led to pore blockage within PVC structure which in turn decreases the porosity as well as permeate flux of the membrane. These results are shown in Table 5.2. Energy-dispersive X-ray spectroscopy data as shown in figure 5.1 verified the presence as well as the dispersion of HB within the membrane. EDX data of M1 shows the presence of C, O and Cl in pristine membrane and addition of HB was easily detected in the plots of M2-M5 with higher intensity of Si, Al with an increased amount of HB.EDS data for samples is shown in table 5.2.

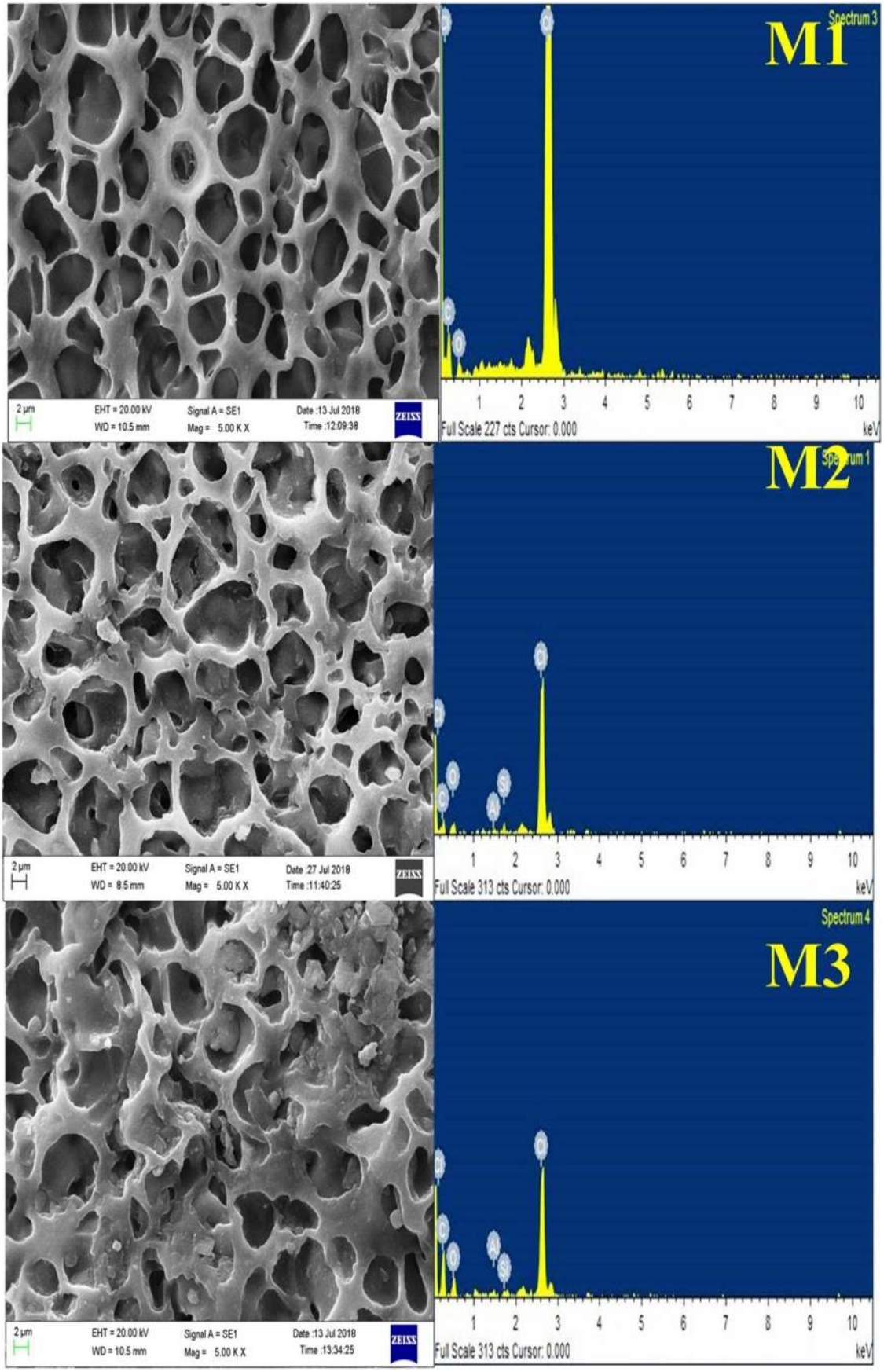

Figure 5.1a: Surface morphology of the top surface of membranes and Energy-dispersive X-ray spectroscopy data for membranes M1-M3.

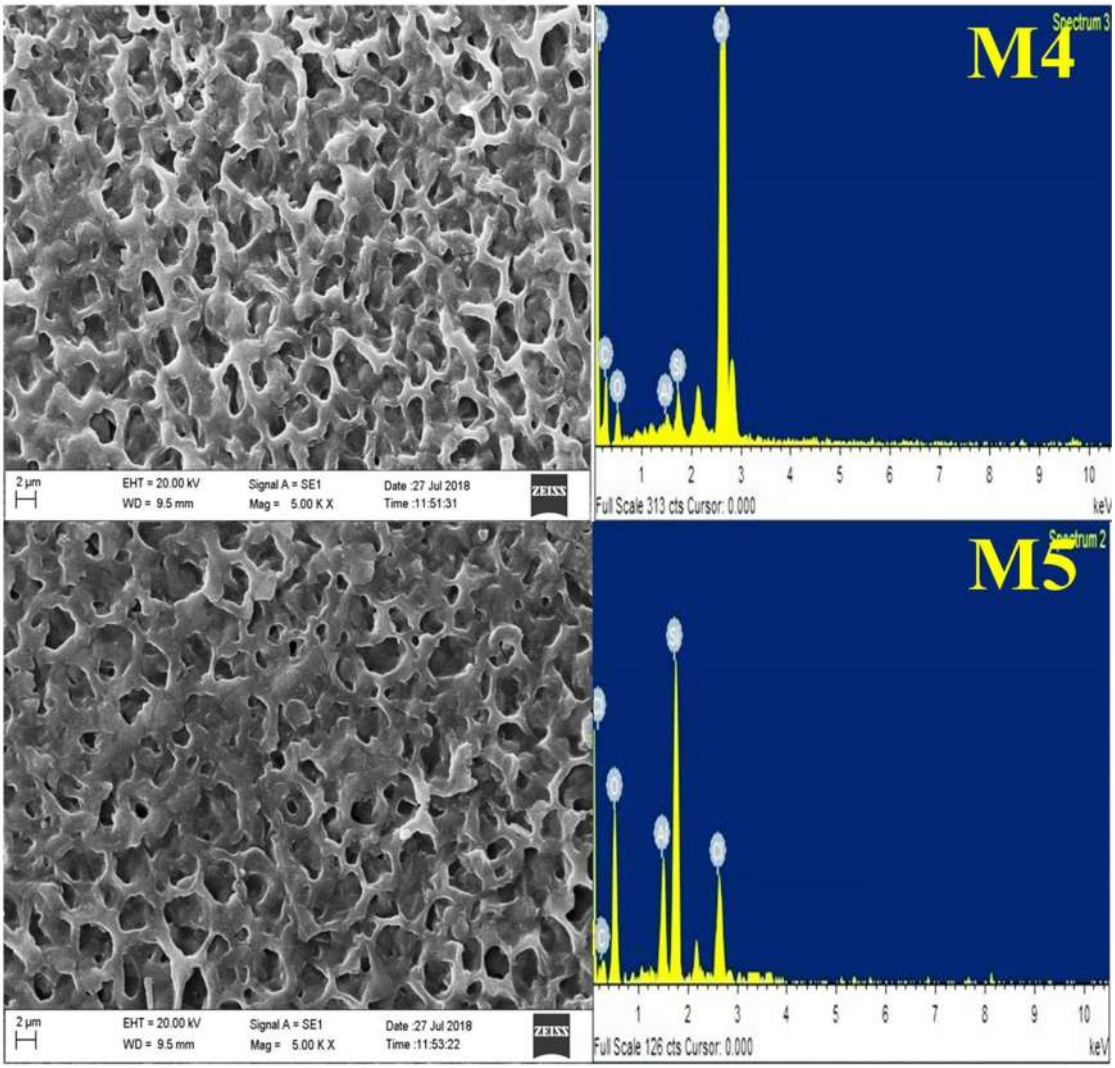

Figure 5.1b: Surface morphology of the top surface of membranes and Energy-dispersive X-ray spectroscopy data for membranes M4 and M5.

Table 5.2: EDS data for membrane samples

Element (Wt%)	M1	M2	M3	M4	M5
C	35.4	32.30	56.76	28.30	54.75
O	9.80	24.10	9.08	18.10	6.87
Al	-	0.65	0.52	0.35	21.05
Si	-	0.98	0.40	1.40	9..39
Cl	54.80	41.87	33.24	51.85	7.94

5.3.2 Thermal Gravimetric analysis

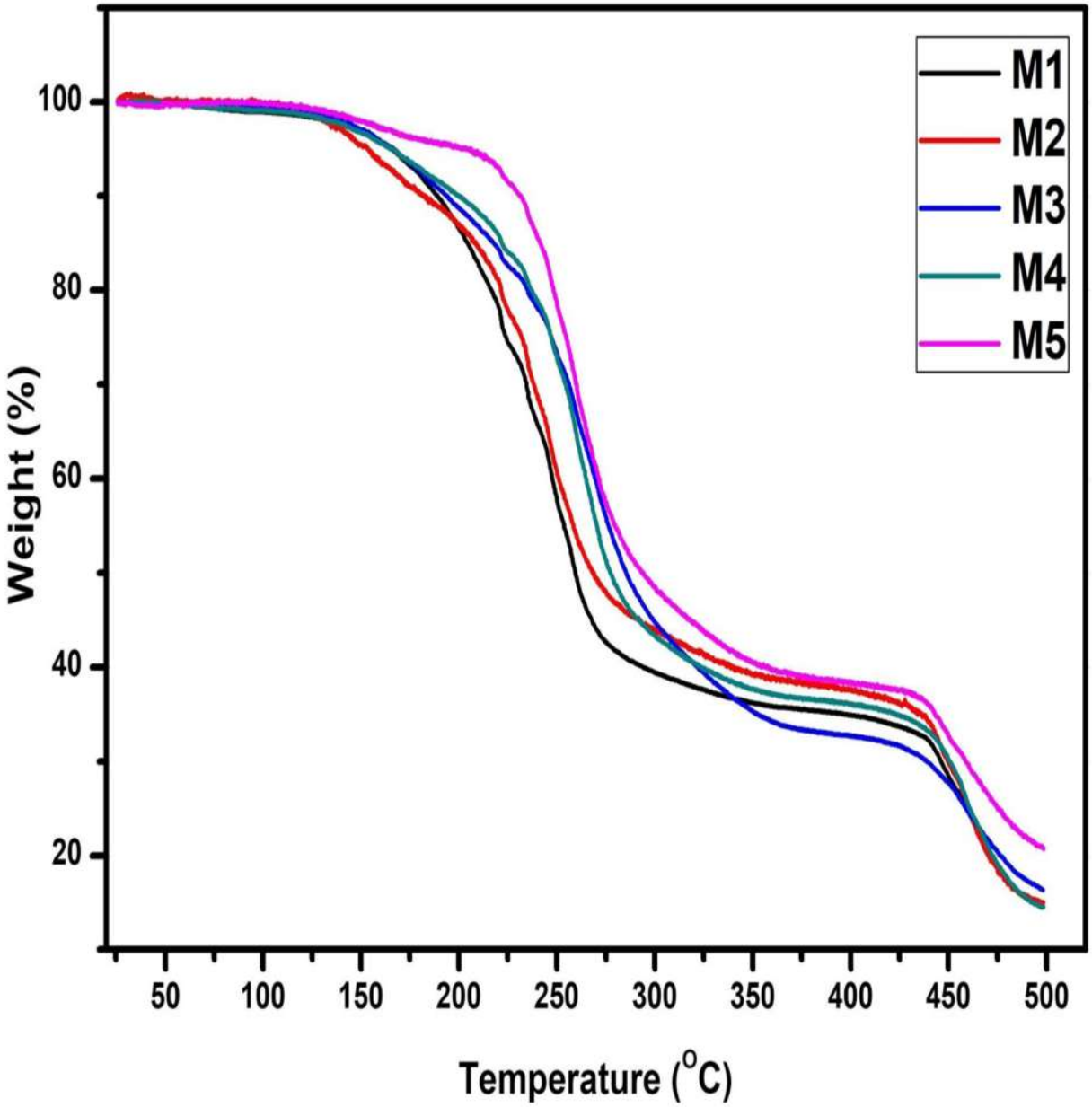

Figure 5.2: Thermal gravimetric analysis of membranes.

Thermal gravimetric analysis was done to compare the thermal stability of pure and composite membranes. TGA graphs of unmodified PVC and alumina composite membranes were recorded with a thermal gravimetric analyzer from room temperature to 500^{o}C and are shown in figure 5.2. For comparison, total degradation between 25-500 ^{O}C is divided in four zones viz. 25-140 ^{O}C, 140-275 ^{O}C, 275-450 ^{O}C and above 450

^{O}C. From room temperature to 140 ^{O}C all samples were stable and showed a very less weight loss of 2-4% because of high melting point of PVC. Major degradation took place between 140-275 ^{O}C where membrane samples showed a high weight loss of 40-55% in this temperature zone. As the temperature reaches 275 ^{O}C, membrane M1 lost 58.22% of its original weight while membrane M5 was more stable and lost 43.27 % of its original weight. A very less degradation of almost 10-14% was observed in comparatively large temperature range of 275-450 ^{O}C. Beyond 450 ^{O}C high degradation was observed and all samples lost almost 85% of their original weight till 500 ^{O}C. These results showed that due to presence of bentonite nanoparticle, thermal stability of composite membranes was increased.

5.3.3 XRD analysis

The presence of HB particles can also be verified by XRD analysis. XRD patterns of pure PVC membrane, pristine HB particles and HB doped membranes are shown in figure 5.3. All peaks appeared to be broad peaks that confirms the amorphous nature of the material which was expected too for polymeric membrane while pristine HB particles give strong diffraction crystalline peaks which is a common structure for inorganic particles. The diffraction patterns of 0.5% HB grafted membrane show a slight shifting of peaks towards the low Theta angle confirming the presence of inorganic material. Similar results were obtained for 1.0%, 1.5% HB grafted membrane i.e. M3, M4 respectively. However for the M5 two more peaks were also observed in the diffraction patterns which were because of the high amount of HB particles present in M5 membrane. Major peaks obtained for membrane samples and pristine HB is shown in table 5.3.

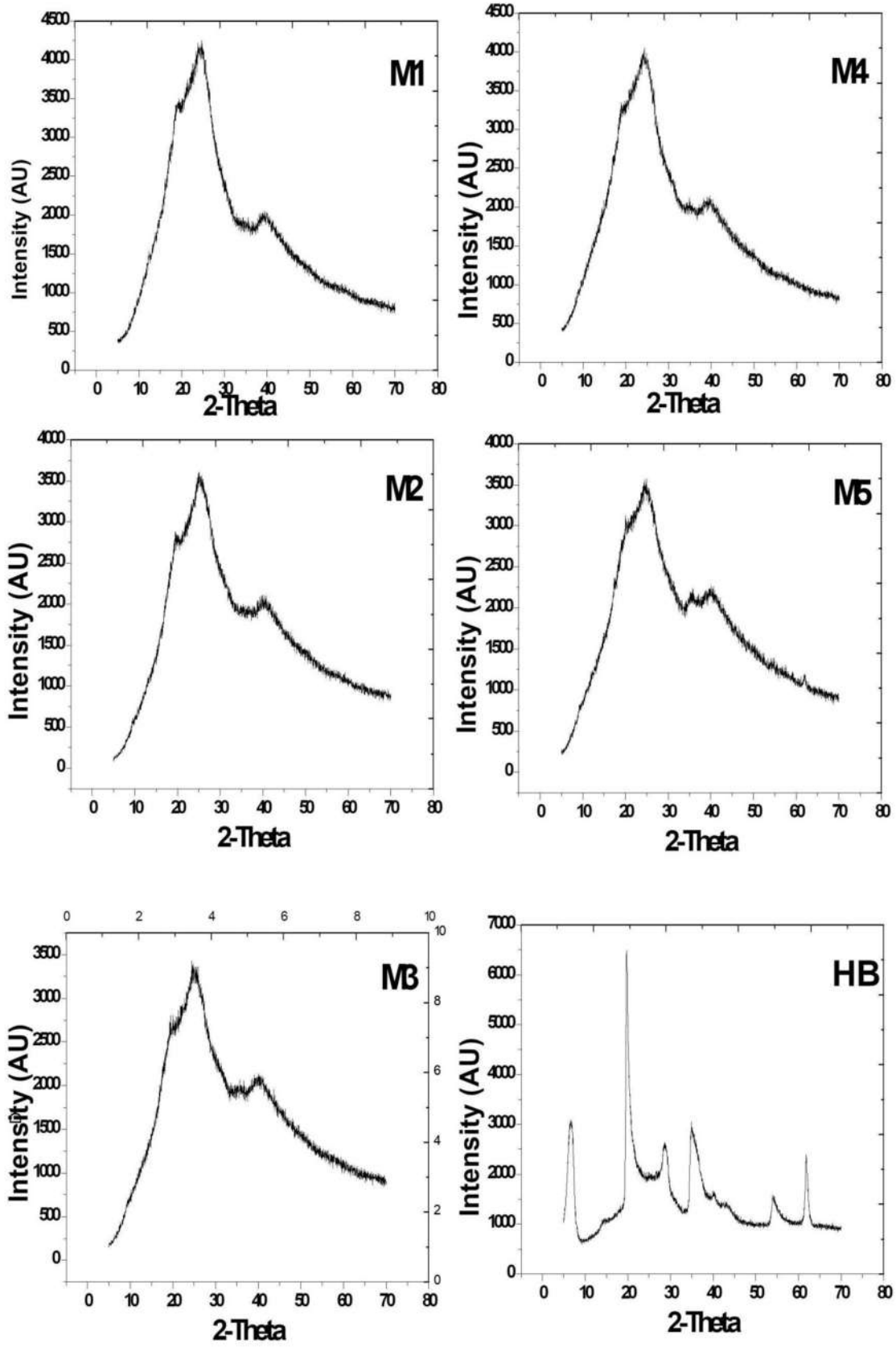

Figure 5.3: XRD patterns of pure PVC membrane, pristine nano bentonite particles and bentonite composite membranes M1-M5.

Table 5.3: Major peaks obtained in membrane samples and pristine HB

Membrane	MAJOR PEAKS (2 THETA)
M1	18.86,24.37,40.05
M2	18.34,23.2,40.08
M3	19.24,24.66,39.84
M4	18.95,24.26,39.81
M5	20.19,25.17,35.58,39.97,62.06
Pristine HB	6.88,19.81,28.64,34.68,53.99,61.84

5.3.4 Mechanical Properties

Mechanical properties are essential characteristics of a membrane as they show the long-term stability for the performance of membrane at high pressures. Incorporation of inorganic materials improved the tensile strength of the material but as the agglomeration of particles took place with higher amount of HB and with the increase of viscosity of polymer blocking of pores took place which in turn reduced the flexibility of the material by decreasing the porosity and make the material more brittle and decreased the tensile strength as well as elongation at break. Data of mechanical properties for composite membrane is given in table 5.4.

5.3.5 Contact angle analysis

The contact angle is the critical characteristic of the membrane which expresses the hydrophilic or hydrophobic nature of the membrane. Lower contact angle values show the strong hydrophilicity of the material. Pure PVC membrane M1 shows the highest contact angle at 73.6^{O} and as the hydrophilic bentonite was added to the polymeric solution the composite membrane showed a lower contact angle. As shown in table 5.4, as the HB amount was increased from 0 to 2%, the contact angle decreased from 73.6 to

51.6^{O} which shows that the hydrophilicity of the membrane surface was enhanced with the addition of hydrophilic Bentonite. Such increase in hydrophilicity of membrane surfaces by adding inorganic material was also reported in various reported literature.

Table 5.4: Tensile stress, elongation, contact angle, porosity and mean pore radius values of the membrane samples.

Membrane	Tensile Stress (kg/cm^2)	Elongation at break (%)	Contact Angle (Degree)	Porosity (%)	Mean pore radius (nm)
M1	66.83 (±2.4)	8.62 (±0.7)	73.6 (±3.1)	66.83 (±1.6)	22.41 (±0.8)
M2	69.65 (±2.2)	9.31 (±0.5)	69.2 (±1.9)	69.65 (±1.8)	25.06 (±1.2)
M3	76.16 (±2.7)	9.74 (±0.6)	62.3 (±2.3)	76.16 (±1.7)	26.38 (±0.9)
M4	73.27 (±2.4)	8.92 (±0.4)	55.2 (±1.6)	73.27 (±2.2)	25.22 (±1.3)
M5	71.39 (±3.1)	7.86 (±0.3)	51.6 (±1.3)	71.39 (±1.9)	24.87 (±1.1)

5.3.6 Porosity and Mean pore radius analysis

Porosity was measured by the 24-hour water retention test. As discussed in the section 4.3.5, porosity of membrane was created by leaching of PVP from polymer solution into water and vicinity created by bentonite particles within the membrane structure around them. It was observed in experiments that porosity of composite membranes increased initially with increasing bentonite concentration in polymer matrix. Due to agglomeration of nanoparticles at high concentration, porosity decreased in M4 and M5. Highest porosity, 76.16% was observed in M3 membrane containing 1 wt% nano bentonite. Guerout–Elford–Ferry (GEF) equation was used for calculation of mean pore radius of the membrane, and it was found that all membranes had mean pore

radius in the nano range between 22-27 nm. Data for porosity and mean pore radius has been given in table 5.4.

5.3.7 Performance studies

After the initial pure water flux measurement $J_{0,}$ the membrane system was subjected to the humic acid solution and flux for each membrane was calculated. Values of J_0, J_P, $J_{1,}$ and J_2 were calculated for all three types of feeds containing 10, 20 and 40 mg/L HA solution and shown in figure 5.4. For each feed fresh membrane was used for filtration so that the comparison of fluxes could be done properly. It was observed that flux for humic acid was lower than the pure water flux due to presence of humic acid particle in the feed stream, which creates extra resistance to membrane and decreases the flux.However, flux for humic acid solution of M_2 is much higher than the neat PVC membrane M1. The higher flux values of M_2 were because of changing pore size and hydrophilicity. Such change in flux relative to pore size and improved hydrophilicity was also observed by Ghazanfari et al. in their study (Ghazanfari et al., 2017). It also increased with increasing content of HB in M_3 and started decreasing in M4 and M5. This improved flux of M2, M3 was the result of improved hydrophilicity and total pore area of membrane but because of particle agglomeration took place with higher concentration of HB, which in turn results in pore blockage which decreases the total pore area through which water passes through the membrane from feed side to permeate side.

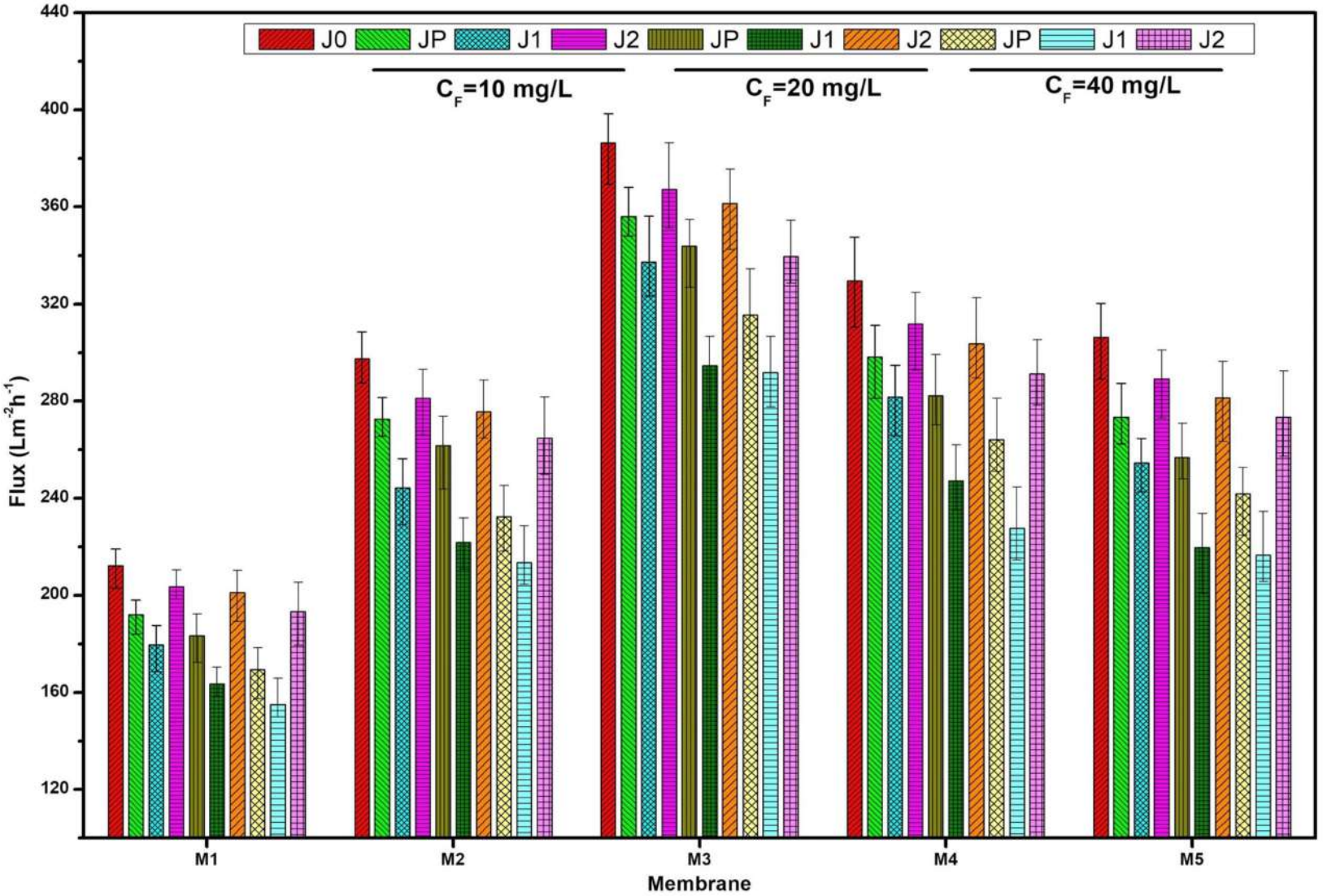

Figure 5.4: Pure water fluxes and permeates flux for feed conditions 10mg/L, 20mg/L and 40 mg/L Humic acid solution

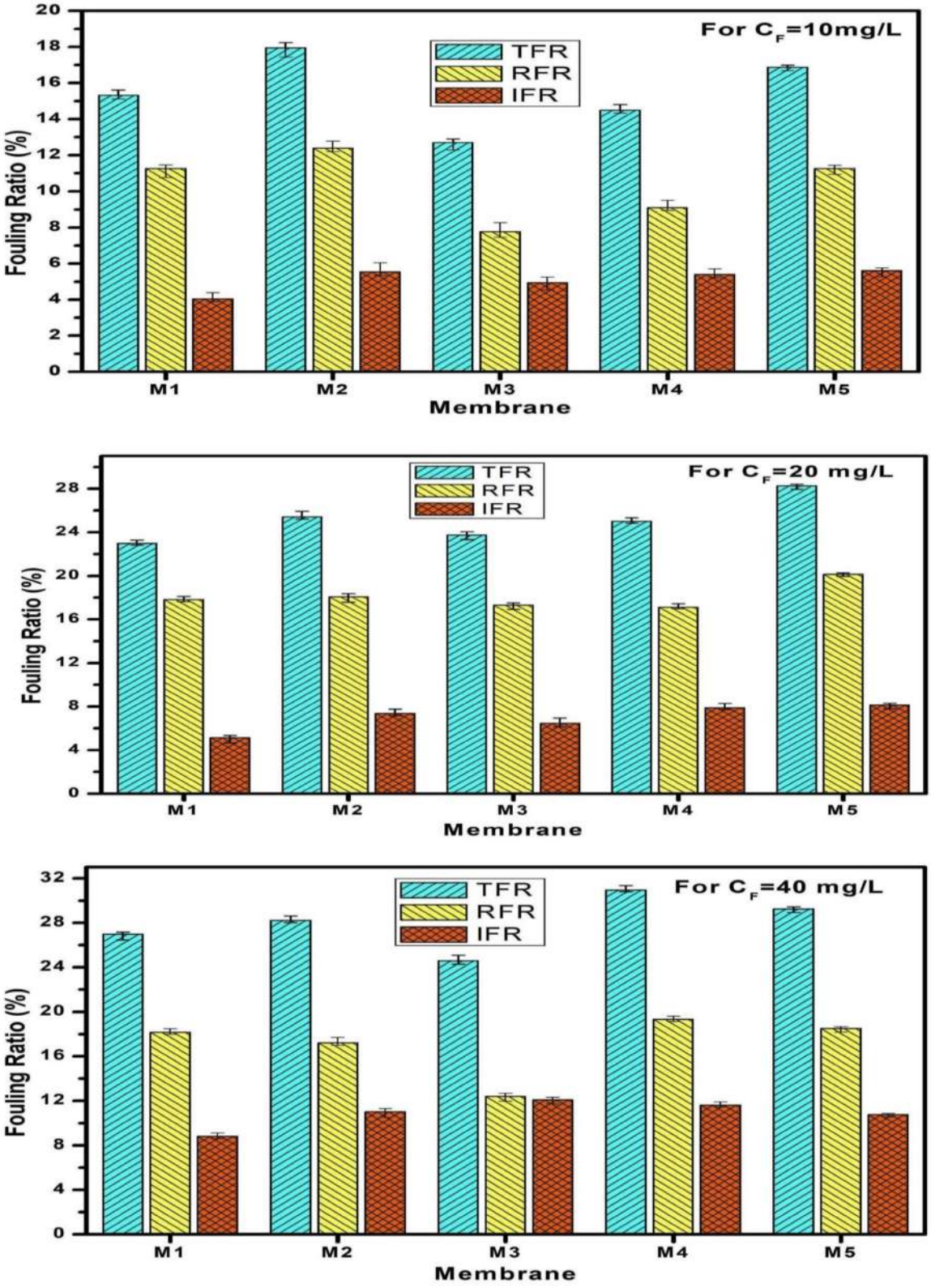

Figure 5.5: Fouling ratio for 10 mg/L, 20 mg/L and 40 mg/L Humic acid solution

In a separate study similar pattern was found by rabiee et al. (Rabiee et al., 2014) by using TiO_2 nanoparticle as filer to prepare composite membrane and they found that at high TiO_2 content, nanoparticles may cause pore blockage of the membranes, which leads to lower water flux. Flux through the membrane directly depends on this area, so as the pore area decreased flux start declining in M4 and M5. A similar pattern was also observed for calculating J_1 and J_2. Flux values were highest for M3 but lower values were obtained for M4 and M5. Still these were much higher than neat PVC membrane M_1. So it can be conclude that the addition of HB improves the flux of membrane relative to neat membrane M1 and optimum performance was found at HB concentration 1% which was also supported by morphological studies.

As the total HA content is increased in feed solution to 20 and 40 mg/L, it was observed that flux declined to lower values for every situation. As the concentration is increased, more foulant was restricted by the membrane at feed side. This may increase resistance of membrane filtration due to pore blockage as well as concentration polarization due to formation of cake layer. After cake layer removal and backwashing when membranes were subjected to pure water. Again, it was shown that pure water flux J_2 at this condition is slightly lower to J_0. However, this flux was still much higher than the flux J_1 for all three feed conditions.

5.3.8 Fouling parameter study

Membrane fouling is expressed as either reversible or irreversible fouling but TFR, RFR and IFR were the parameters to express the fouling behavior of membrane. Values of TFR, RFR and IFR were measured in all three feed conditions and shown in figure 5.5. For feed concentration 10 mg/L membrane M3 has shown lowest fouling as it was expected for this

sample. Major fraction of fouling was because of reversible fouling which was 73.53%, 69.10%, 61.01%, 66.76% and 66.73% of total fouling of membranes M1-M5 respectively. Irreversible fouling, however, was highest for the membrane M3. Few researchers have also reported such change in total fouling while studying performance of composite membranes (Behboudi et al., 2016; Taghaddosi et al., 2017).

For 20 mg/L feed sample, total fouling was higher than 10 mg/L feed for all membrane samples. It was expected because of higher amount of foulant would make a thick layer of cake on the feed side membrane surface and increase the resistance created because of concentration polarization. However, here most of the fouling was reversible as the cake was removed and membrane was back washed. Reversible fouling for this condition was ranged between 68-77% of total fouling for all five samples. Absolute values of irreversible fouling were also observed higher for 20 mg/L as compared to 10 mg/L, which showed that some small pores were blocked more easily in the presence of higher amount of foulant available in feed (Kusworo et al., 2018). Similarly, for feed 40 mg/L, we found the same pattern that total fouling, as well as irreversible fouling, increased. All membranes showed the major role of reversible fouling in creating total fouling except members M3. This membrane showed almost equal ratio of both fouling types in total fouling. This membrane showed higher reversible fouling because of smaller range of pores which were easily fouled by foulant.

5.3.9 Rejection rate

The primary aim of any filtration operation is to filter out maximum possible targeted particle from the feed solution. For study of the membrane performance, rejection rate was calculated using equation 3.12. Data obtained by calculations are shown in figure 5.6 for all three feed conditions respectively. The highest rejection was observed for M3 membrane in 10 mg/L feed condition. Since mean pore size of M3 is smallest, so it was obvious for this membrane to show the maximum rejection rate. A similar pattern was found in next two feed condition but this time rejection rate declined. Increased total fouling could be the main reason for this decrease in rejection rate.

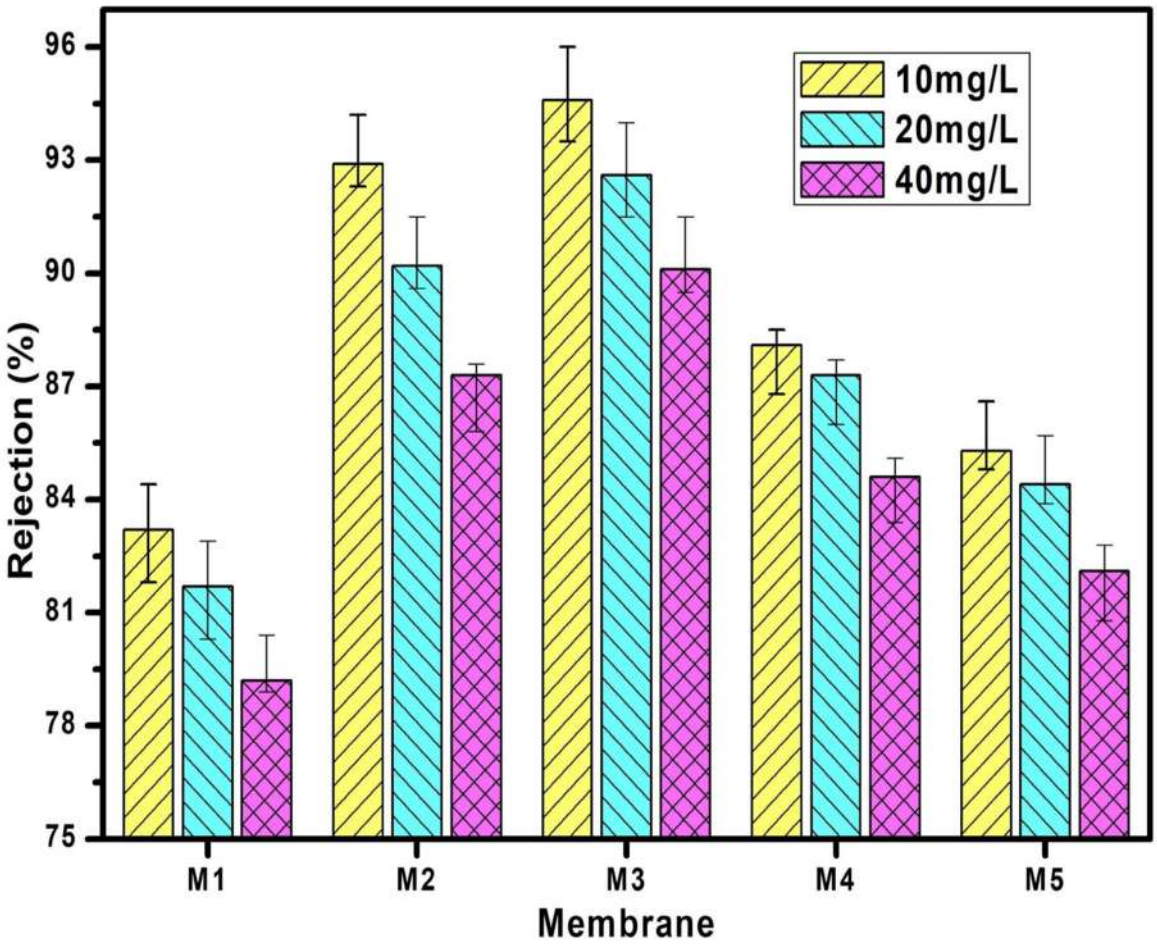

Figure 5.6 Rejection for 10 mg/L, 20 mg/L and 40 mg/L Humic acid solution

5.3.10 Flux recovery

Another parameter to study fouling, i.e., flux recovery was also calculated using equation 3.7 and shown in figure 5.7. Flux recovery is reversely proportional to irreversible fouling. Higher irreversible fouling result in low recovery and lower irreversible fouling reflects the higher flux recovery (Ghazanfari et al., 2017; Wu et al., 2015). Ghazanfari Et al. reported that the flux recovery increased from 69% to 86% when the filler content was increased in base composite membrane. As the reversible fouling is increased with high amount of humic acid in feed, flux recovery also declined. For condition 10 mg/L, it was highest for membrane M_1 and valued for 95.93% and reduced to 94.86% and 91.18% for feed 20 mg/L and 40 mg/L respectively.

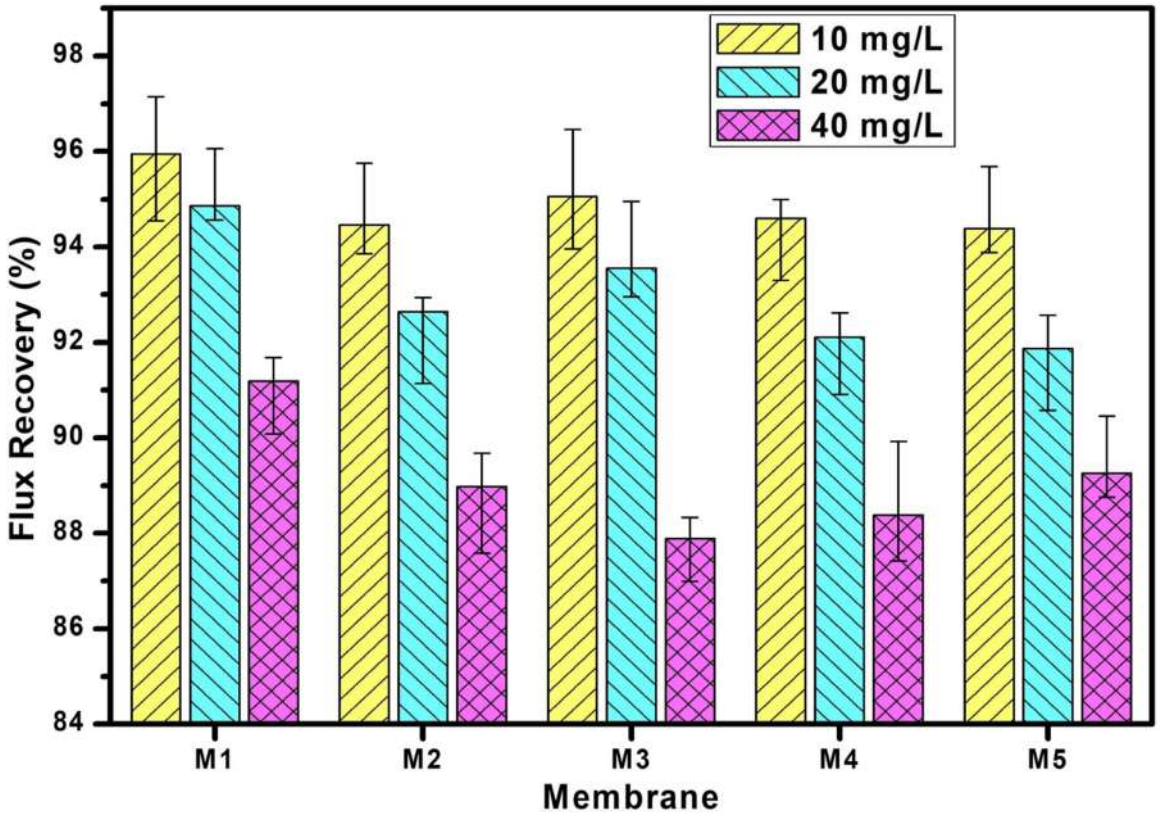

Figure 5.7: Flux Recovery for 10 mg/L, 20 mg/L and 40 mg/L Humic acid solution

5.3.11 Relative Flux

Relative flux is a parameter to observe how flux varies through a membrane when it is subjected to real operation as compared to pure water flow. This is a fractional value and ratio of flux of humic acid solution to pure water flux (Maximous et al., 2009). As it is shown in figure 5.8, for 10 mg/L solution relative flux varies between 0.89-0.92.0.92 was highest relative flux for membrane M3. But as the amount of humic acid was increased in feed, flux through the membrane decreased because of various resistances provided by membrane and cake layer to the flow. For 40 mg/L feed solution, relative flux dropped to a vary law value 0.79 for membrane M5.

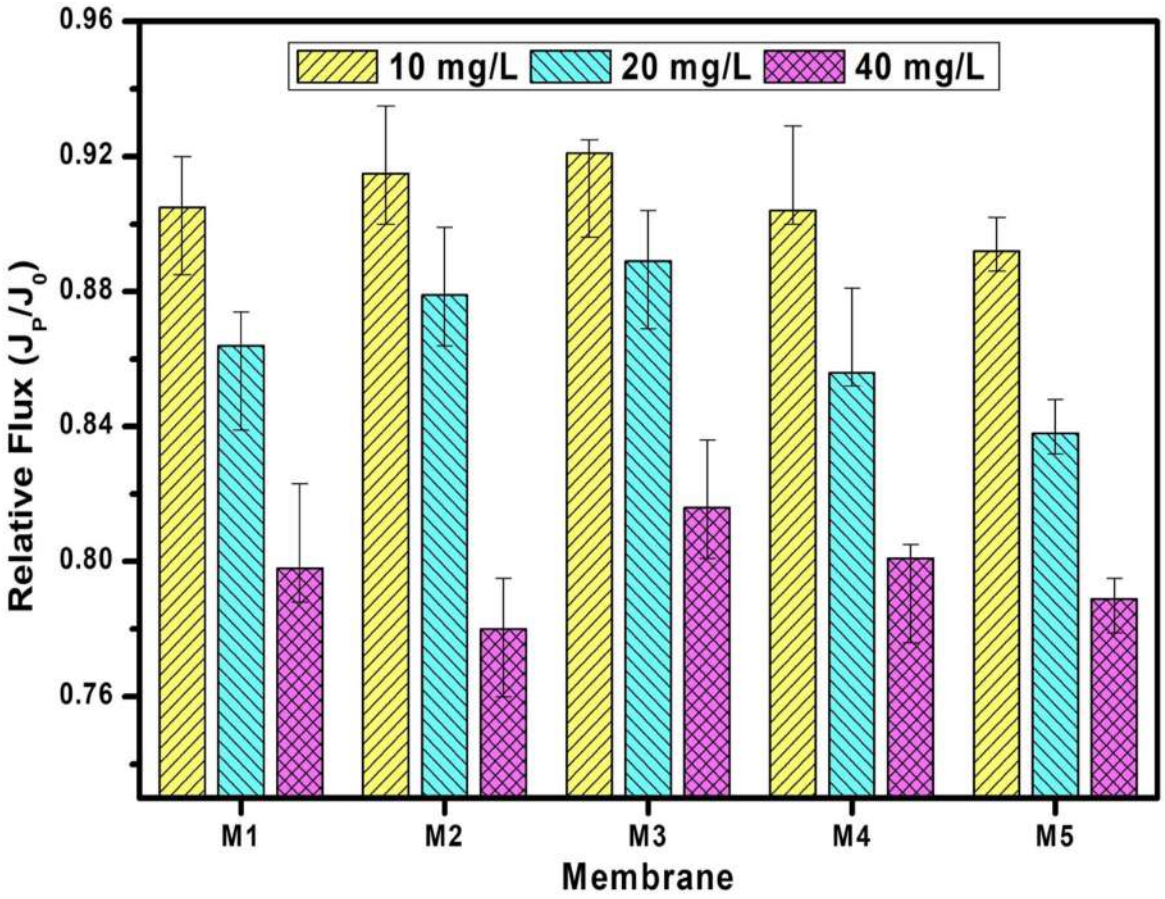

Figure 5.8: Relatives flux of the membranes for 10 mg/L, 20 mg/L and 40 mg/L Humic acid solution

5.3.12 Membrane resistance

Membrane resistance to the separation process was calculated by the equations 3.8- 3.11 as discussed in the section 3.3 and plotted as shown in figure 5.9. Antifouling nature of composite membrane M3 was also verified by this parameter. It can be observed that irreversible fouling resistance and resistance due to concentration polarization increased with higher feed concentration and increasing total resistance to separation. Membrane M3 showed lowest resistance to separation in all three feed conditions.

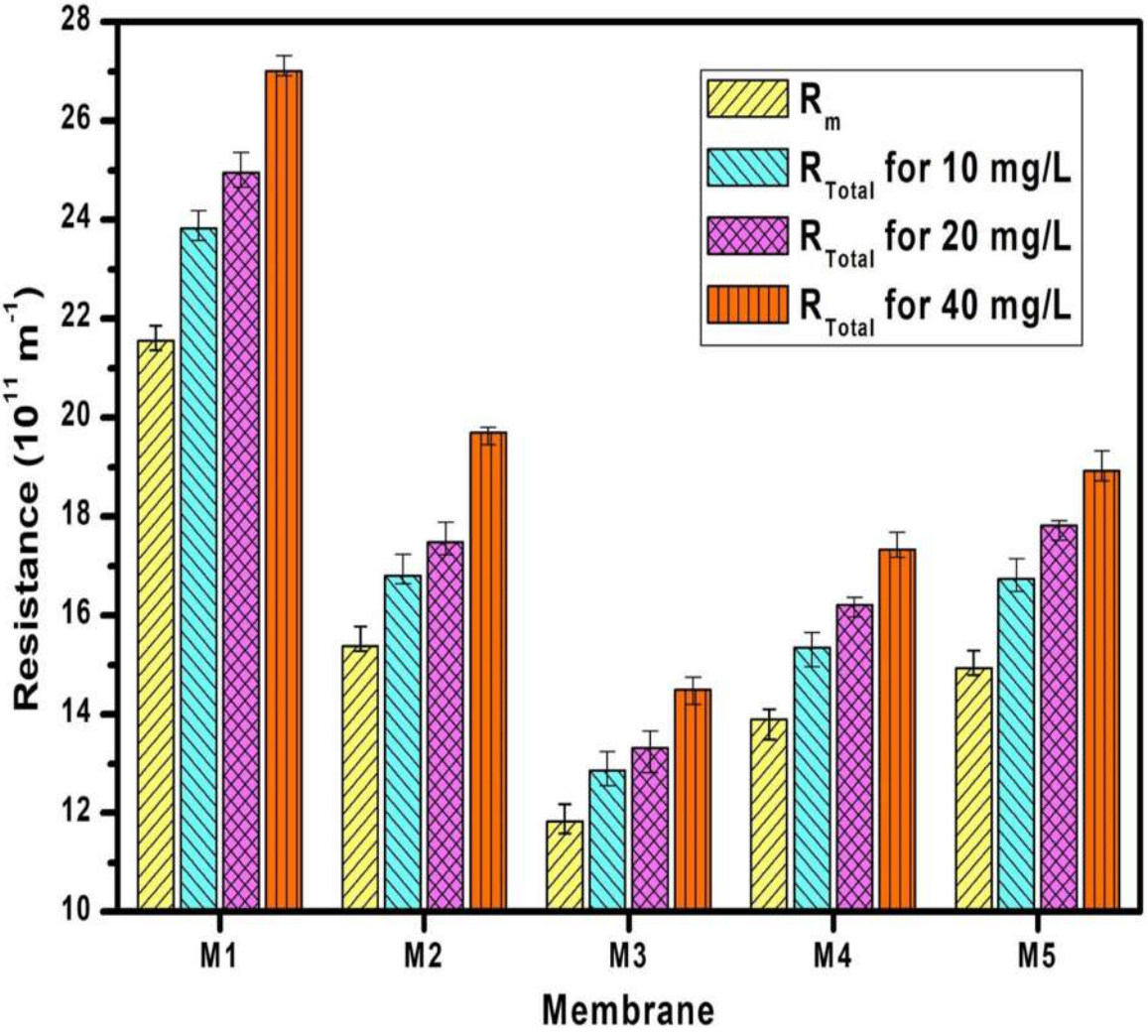

Figure 5.9: Intrinsic and total resistance to membranes for 10 mg/L, 20 mg/L and 40 mg/L Humic acid solution